RREASO Building Structure Physical Parameter Identification Algorithm for Structural Damage Identification

Xin Li
Department of Construction Engineering and Economic Management, Applied Technology College of Dalian Ocean University, Dalian 116300, China
E-mail: 13795170948@163.com

Keywords: structural damage identification, substructure, atomic search optimization algorithm, roulette wheel selection, random walk

Received: May 7, 2024

With the intensification of human modernization, civil engineering and building structures have become increasingly complex. Potential security risks have also emerged. Therefore, scientific structural parameter identification algorithms are particularly crucial for health monitoring of current complex building structures. Therefore, the traditional atomic search optimization algorithm is improved ground on the roulette wheel selection strategy, random walk strategy, elite selection strategy, and substructure technology. The numerical simulation experiment results showed that the improved method performed better than the atomic search optimization algorithm in identifying structures with more degrees of freedom. The maximum relative errors for substructure and full structure stiffness identification were 13% and 43.1%, respectively, indicating that the combination of the improved algorithm and substructure identification method had better structural parameter identification results. In real structural parameter identification experiments, the identification error of the improved algorithm was less than 10%, the identification stiffness was reduced to 58.9%, and the relative error was around 10%, which was better than the traditional atomic search optimization algorithm. This indicates the effectiveness and feasibility in identifying building structural parameters, which is essential to ensure the safety and durability of real engineered structures.

Povzetek: Predlagan algoritem RREASO za identifikacijo fizikalnih parametrov strukture stavb, ki temelji na optimizaciji atomske iskalne metode, izboljšuje identifikacijo strukturnih poškodb s strategijami rulete, naključne hoje in izbire elit.

1 Introduction

The rapid growth of the social economy and industrial technology has led to the emergence of many super high-rise buildings, large-span bridges, and spatial structures in civil engineering. These infrastructure facilities are developing towards large-scale, complex, and intelligent development to meet the needs of material life and industrial construction. Civil engineering structures are exposed to complex environments for a long time and are subjected to the coupling effects of loads and various external accidental factors, which inevitably leads to stiffness degradation or damage accumulation in the structure [1, 2]. However, the damage to the civil engineering structure has seriously affected the development of the national economy. If it is possible to regularly or in real-time inspect complex building structures and conduct risk analysis on them, corresponding measures can be taken to reduce or avoid accidents. Therefore, structural health monitoring has become one of the hot research topics in the civil engineering. Structural parameter identification is the foundation of structural health monitoring [3, 4]. Structural parameter identification is an important step in the health monitoring process. Recently, more scholars have applied various algorithms to parameter identification in building structures. For example, Dinh proposed a structural parameter identification method for damping structures. Compared with other parameter identification methods, this method had lower computational cost and higher detection dimensions [5]. Zhang et al. proposed a frequency domain non-iterative method for parameter identification of shear type building structures under earthquake action. This algorithm used modal information represented by spectral ratio to greatly improve estimation accuracy [6]. Machine learning and deep learning algorithms have also been extensively studied in the identification of structural parameters. For example, Bao et al. proposed a deep transfer learning network for structural state recognition ground on limited real-world training data. The embedded knowledge was transferred to real monitoring/testing [7]. Zhang et al. integrated pattern recognition and finite element model correction. This method used physics-based machine learning to identify structural damage [8]. Combining continuous wavelet transform and deep convolutional neural network, Lu et al. proposed a new sensor

data-driven structural damage detection method to improve the robustness [9]. Fallah et al. proposed a new comprehensive machine learning model for predicting two energy parameters of residential buildings and analyzing building characteristics [10]. Elghaish et al. developed a new deep learning convolutional neural network to classify highway cracks [11]. In the identification of building structural parameters, Malekkhaini et al. built a two-step finite element correction method for health monitoring of prestressed concrete beam bridges [12]. Funari used a generative programming paradigm to implement the modeling framework into a visual programming environment. Furthermore, a new parameter scanning finite element method suitable for architectural heritage was proposed [13].

Traditional iterative and gradient methods have high computational complexity, difficulty in selecting initial values, and weak global search capabilities. Therefore, Han et al. developed a parameter identification method ground on the Atomic Search Optimization (ASO) to address this issue [14]. Wangdeng et al. proposed an improved artificial hummingbird strategy. It was used for parameter identification of pumped storage units, improving the global search ability of the initial population [15]. Asna et al. proposed an effective method for planning fast charging stations for electric vehicles ground on the ASO, which improved the convergence speed of the algorithm [16]. Eker et al. integrated artificial fish swarm algorithm with simulated annealing algorithm. It was applied to multi-layer perceptron training and motor speed control. The algorithm was successful for optimization problems with different properties [17]. Bi et al. proposed an improved grey wolf algorithm for optimizing multi-layer perceptron recognition of plant diseases. It could effectively avoid local optimization as well as premature convergence [18]. Table 1 summarizes the research ideas and shortcomings of previous scholars on building structures, damage identification, and other related topics.

Table 1: Summary of related work on identification of structural damage and related parameters in building structures

Scholar	Methodology	Key results	Limitations
Dinh [5]	Identification method for damping structure parameters	Low computational cost and high detection dimension	Difficulty in considering other changes in the building structure
Zhang et al. [6]	Non iterative algorithm for parameter identification of shear type building structures	Improved estimation accuracy and reduced human intervention	Restricted data selection properties
Bao et al. [7]	Deep transfer learning network based on structural state recognition	High training data monitoring effect	It may be difficult to handle non-linear structured data types well
Lu et al. [8]	The combination of sensor data-driven and deep convolutional neural networks	High accuracy and robustness in damage detection	Low data processing efficiency
Fallah et al. [9]	Using comprehensive machine learning models to predict building energy parameters	Better recognition effect for building features	The applicability of the method may be limited by region
Elghaish et al. [10]	Deep learning convolutional neural network model for detecting and classifying highway cracks	Significant application effect	The feature detection effect of highway cracks in different environments is poor
Malekkhaini et al. [12]	Health monitoring and damage identification of concrete beam bridges using a two-step finite element model	High accuracy in damage detection	The rationality of data selection is difficult to ensure
Funari [13]	Using generative programming paradigm to scan building parameters in modeling framework	Scanning characteristics of building parameters that are relatively consistent with actual values	Low accuracy in selecting subtle building parameters
Han et al. [14]	Atomic search algorithm identification parameters	Improved global search capability	Restricted operational efficiency

Wang et al. [15]	Improved artificial hummingbird algorithm for identifying the parameters of the speed control system of pumped storage units	Improved global search ability for the initial population	The calculation resource consumption of the speed control system is relatively high
Asna et al. [16]	Multi-objective binary version ASO algorithm for planning automotive charging stations	Improved algorithm convergence speed	Difficulty in considering the energy consumption utilization of car charging stations
Eker et al. [17]	Integrating artificial fish swarm algorithm and simulated annealing algorithm to control motor Speed	High applicability	Performance testing may be significantly affected by scene detection
Bi et al. [18]	Improved grey wolf algorithm for optimizing multi-layer perceptrons	High accuracy in plant disease identification, avoiding local optimization problems	The accuracy of the algorithm is significantly affected by the size of the data volume

At present, scholars have conducted extensive research on the problems related to the identification of building structure parameters, among which the ASO algorithm has been successfully applied to this area. It can improve the global search ability of the initial population and plan for fast charging of electric vehicles. However, the traditional ASO algorithm can easily fall into the local optimal or identify the structure parameters of the higher degree of freedom. Therefore, the study uses the roulette selection strategy, random walk strategy and elite selection strategy to optimize the selection mode of atomic search path. Combined with substructure technology, an improved ASO algorithm is proposed to improve the accuracy and computational efficiency for parameter identification of complex architectural structures.

The study is divided into four parts. The first part summarizes the background and related research on identifying building structural parameters, providing a theoretical basis for the following text. The second part is to elaborate on the improved ASO. The third part is to verify the effectiveness of the RREASO ground on real structural parameter identification experiments. The last part summarizes the entire text.

2 Method and materials

A structural parameter identification method based on ASO is designed. Combining substructure technology, the roulette wheel selection strategy, random walk strategy, and elite selection strategy are introduced into the ASO to improve the algorithm.

2.1 Structural parameter identification based on ASO

Structural parameter identification is achieved through structural dynamics system identification technology. By utilizing the input and output information of the structural system, a mathematical model equivalent to the actual structural system is constructed. The unknown parameters in the model are solved [19]. The key is to define the equivalent standard of the system. The error function of the standard implementation is shown in formula (1).

$$Y = Y\left(X_a(\theta), X_m\right) \tag{1}$$

In formula (1), X_a signifies the output of the analysis model. Y represents the error function. X_m represents the actual output of the actual structure. The main content of structural parameter identification includes two parts: optimization algorithm and parameter estimation criterion. At present, the least squares criterion is the most widely used parameter estimation criterion. Considering the complexity of the structure, constraints will be added when using optimization algorithms in practice. The objective function is composed of constraints and error functions, as shown in formula (2).

$$Q = Y\left(X_a(\theta), X_m\right) + \sum_{i=1}^{n} \alpha_i M_i \tag{2}$$

In formula (2), Q signifies the objective function. α_i signifies the weight coefficient. M_i represents the scalar error generated by the i-th constraint equation. After considering the constraint conditions in the objective function, the structural identification parameter problem is transformed into a constraint optimization problem. Its optimization model is shown in formula (3).

$$\begin{cases} \min Q(\theta), s.t. \theta \in \{S\} \\ y(k) = f\left(u(k), \theta\right) \end{cases} \tag{3}$$

In formula (3), y signifies the output of the system. θ represents the system parameters to be identified. u signifies the input. t signifies the discrete time point. The objective function to minimize the error in the actual measured structural output and the input of the alternative analytical model at this point is shown in formula (4).

$$F(\theta) = \frac{1}{T}\sum_{k=1}^{T} \left\| y(k) - \hat{y}(k) \right\|^2 \tag{4}$$

In formula (4), T represents the sampling time point. The optimization problem finds a suitable θ to minimize $F(\bullet)$. In the ASO algorithm, the identification problem is handled as a linear multi-dimensional optimization problem, as shown in formula (5).

$$\min F(\theta), \theta = (\theta_1, \theta_2, ...\theta_n) \quad (5)$$

In formula (5), the lower limit $\theta_{\min}$ and upper limit $\theta_{\max}$ of the parameter n to be identified constitute the search space of the ASO.

2.2 Structure based on RREASO parameter recognition

The ASO algorithm performs very well in solving low dimensional problems. However, as the dimensionality of the problem increases, the problem becomes more complex, which makes the drawbacks of ASO more apparent and the recognition results are not ideal. Moreover, civil engineering structures are complex and have a high degree of freedom. The parameter identification problem can be transformed into high-dimensional and more complex nonlinear optimization. When dealing with such parameter identification, structural parameter identification methods based on ASO algorithm are prone to getting stuck in local optima. In response to this limitation, the study adopts roulette wheel selection, random walk, and elite selection strategies to increase randomization features to maintain population diversity, allowing particles to continuously explore unknown regions. The improved ASO algorithm is named RREASO.

In the ASO algorithm, the roulette wheel selection strategy first calculates the fitness value Fit_i for each atom. According to the calculated results, atoms are sorted. The probability Pi of atoms is calculated, as shown in formula (6).

$$P_i = \frac{1/Fit_i}{\sum_{I=1}^{N} 1/Fit_i} \quad (6)$$

Secondly, the cumulative probability of each atom is calculated to construct the roulette wheel, as shown in formula (7).

$$q_i = \sum_{i=1}^{N} P(i) \quad (7)$$

In formula (7), Pi signifies the probability of the i-th atom being selected. q_i represents the cumulative probability of the q_i-th atom. N represents total atoms. Next, a roulette wheel selection is performed to randomly generate a number in $[0,1]$. If the number is less than q_i, the i-th atom is selected to enter the next ASO algorithm iteration population. The roulette wheel selection is repeated $N/2$ times to select $N/2$ atoms to form a new population. For each selected atom, the position of the atom can be calculated. Assuming that the atom randomly walks around the position of the atom with increasing iterations, the search range of the atom is expanded. The relationship is shown in formula (8).

$$Xi = \frac{(xi - ai) \times (di - ci)}{bi - ai} + C_i \quad (8)$$

In formula (8), di and ci signify the maximum and minimum values of the search space boundary. bi signifies the maximum of the random walk of the i-th variable. ai signifies the minimum of the i-th variable. The ASO algorithm selects the minimum fitness value as the elite value in the elite selection strategy at each iteration, and its corresponding atom is called the elite atom.

In summary, the RREASO first selects $N/2$ better atoms through a roulette wheel selection strategy, and randomly walks the position of the selected atoms. The position after random walking is denoted as R_A. Secondly, the elite atomic positions selected based on the elite retention strategy are randomly walked. The atomic positions after random walking are recorded as R_E. Finally, the average of the two random walk positions is used as the final atomic position, as shown in formula (9).

$$X_i^t = \frac{R_A^t + R_E^t}{2} \quad (9)$$

In formula (9), t represents the number of iterations. X_i^t signifies the position of the i-th atom at the t-th iteration.

2.3 Structural parameter identification of combined substructure method and RREASO

When there are too many parameters to identify in the structure, to further improve the convergence speed and computational efficiency of the RREASO, a divide and conquer approach is proposed. This approach divides the entire structure into several substructures. Each substructure recognition can identify all parameters. The substructure identification method is presented in Figure 1.

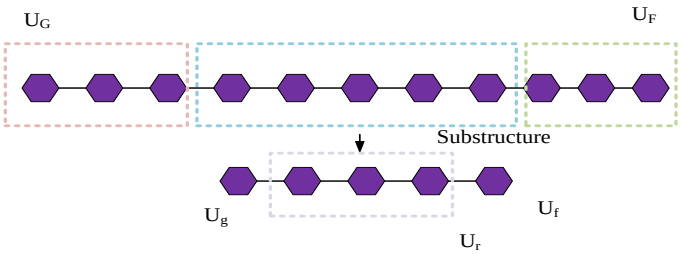

Figure 1: Schematic diagram of substructure identification method

In Figure 1, U represents the displacement generated by the particle. F and G represent the residual structural degrees of freedom on both sides of the substructure. r represents the internal degrees of freedom of the substructure. g and f signify the degrees of freedom at the upper and lower thresholds of the substructure. For the sake of simplicity, e represents all the boundary degrees of freedom. The interaction effects on the boundary of the substructure are taken as inputs to the substructure system. The dynamic formula of the substructure is shown in formula (10).

$$M_{rr}\ddot{U}_r(t)+C_{rr}\dot{U}_r(t)+k_{rr}U_r(t)=\Pr(t)-M_{rr}\ddot{U}_e(t)-C_{re}\dot{U}_e(t)-k_{re}U_e(t) \quad (10)$$

The input of the substructure is the acceleration response signal of the degrees of freedom at the interface of the substructure. In practical engineering, obtaining velocity and displacement through integration can result in errors. Therefore, the accelerometer is usually applied to measure the dynamic response. The study introduces a "quasi-static displacement" vector to eliminate the need for velocity and displacement signals in practice, as shown in formula (11).

$$U_r=U_r^s+U_r^* \quad (11)$$

In formula (11), U_r^s represents the quasi-static displacement vector. U_r^* represents the relative displacement vector. U_r represents the displacement generated by the internal degrees of freedom of the substructure. The quasi-static displacement is the displacement vector generated by the internal degrees of freedom. It is obtained from the inertial effect, ignoring system excitation $\Pr$, and damping effect, as shown in formula (12).

$$U_r^s=-K_{rr}^{-1}K_{re}Ue=rU_e \quad (12)$$

In practical engineering, damping force is smaller compared with inertial force. Therefore, the study assumes that the velocity term in boundary motion is ignored. Combined with the dynamic equations of the substructure, the boundary motion force vector is acquired, as displayed in formula (13).

$$M_{rr}\ddot{U}_r^*(t)+C_{rr}\dot{U}_r^*(t)+k_{rr}U_r^*(t)=\Pr(t)-\ddot{U}_e(t)(M_{re}+M_{rr}r) \quad (13)$$

Once the boundary acceleration signal is obtained, the boundary motion vector can be calculated. The boundary mass matrix M_{re} of the centralized mass system is a zero matrix. Formula (13) can be simplified, as shown in formula (14).

$$M_{rr}\ddot{U}_r^*(t)+C_{rr}\dot{U}_r^*(t)+k_{rr}U_r^*(t)=\Pr(t)-\ddot{U}_e(t)M_{rr}r \quad (14)$$

At this time, the objective function of minimizing the error in the actual measured structural output and the input of the alternative analytical model is updated using the specific collected acceleration signal, as shown in formula (15).

$$F(\theta)=\frac{\sum_{i=1}^{S}\sum_{k=1}^{L}\left\|\ddot{U}_m(i,k)-\ddot{U}_v(i,k)\right\|^2}{SL} \quad (15)$$

In formula (15), v represents the candidate analysis model for identification using the RREASO algorithm. m represents the measured structural system. S represents the acceleration sensor number. L signifies the number of time points collected by the system.

When combining the substructure method and RREASO algorithm for parameter identification, the relative acceleration relationship used for fitness evaluation is shown in formula (16).

$$\ddot{U}_r^*(t)=\ddot{U}_r(t)-r\ddot{U}_e(t) \quad (16)$$

The flowchart of using RREASO to identify substructure parameters is shown in Figure 2.

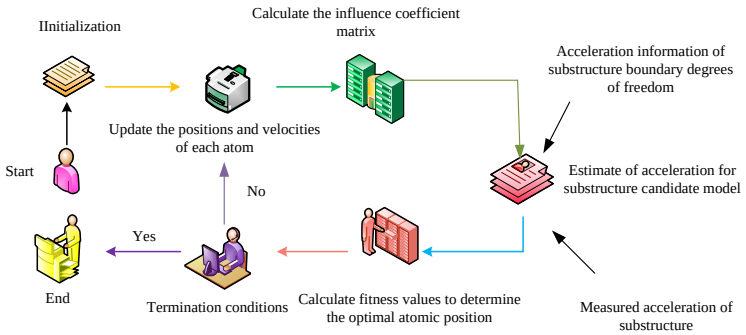

Figure 2: Flow chart of RREASO identifying a substructure parameter

According to the above description, the steps for obtaining the combined substructure method and RREASO algorithm are as follows.

Firstly, the whole structure to be identified is divided into several substructures. A substructure with known acceleration of the boundary degree of freedom is taken for identify. The physical parameters of the substructure are taken as the dimensional components of each atom in RREASO, and the RREASO algorithm is used to identify them. The acceleration of the internal degrees of freedom of the identified substructure can be used as the known boundary acceleration of its adjacent substructures. Then, another substructure with known acceleration of boundary degree of freedom continues to identify, with the required parameters and identification methods consistent with step 2. The substructure acceleration of boundary degree of freedom at this time can be acquired by actual measurements or from the computed acceleration of the previously identified internal degrees of freedom of the substructures. Finally, if the adaptation value function of the RREASO algorithm has converged or reached the maximum number of iterations, the structure parameter identification of the next substructure is entered or ended the recognition. Otherwise, the speed and position of each atomic element in the RREASO are adjusted according to the adaptation value function to enter the next generation update.

3 Results

A numerical simulation experiment for parameter identification of a 10 story and 25 story shear type frames, and a system parameter identification experiment of a five-story metal frame structure are designed to verify the effectiveness and feasibility of the RREASO.

3.1 Numerical simulation of structural parameter identification based on RREASO

Firstly, numerical simulations are conducted on the parameters of a 10-story shear frame. The parameter identification results of the ASO are compared to verify the effectiveness of the RREASO in dealing with structural parameter identification problems with more degrees of freedom. The numerical simulation experiment settings are displayed in Table 2.

Table 2: Experimental setup

Numerical simulation	Term	Value
Floor stiffness(KN/m)	1	2.00E+06
	2	1.96E+06
	3	1.92E+06
	4	1.88E+06
	5	1.84E+06
	6	1.80E+06
	7	1.76E+06
	8	1.72E+06
	9	1.68E+06
	10	1.64E+06
Mode damping ratio	First order	5%
	Second order	12%
Parameter	Time history	10s
	Sampling interval	0.02s
	White Gaussian noise	10%
	Iterations	3000

The objective function established by numerical simulation in Table 2 is the error norm between the acceleration signals output by the real structure and the candidate estimation model. Each operating condition

undergoes 20 independent calculations and the average is the final recognition result. The search space is defined as a true value between 0.5 and 2.0 times. The structural system is a centralized mass system, with the mass of the structure concentrated on each floor slab. It is assumed that the mass of the structural parameters to be identified in the system is known. The structural response information collected in actual engineering may not be complete, this study divides the response information in numerical simulation into two situations: fully measurable and partially measurable. The structural parameter identification results of the ASO and RREASO are shown in Figure 3.

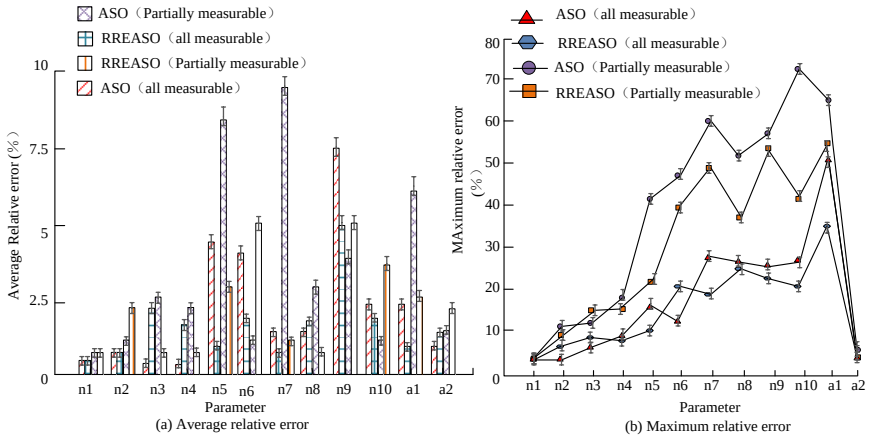

Figure 3: Structural parameter identification results of ASO and RREASO

From Figure 3, the structural parameter identification problem was 12 dimensions. The average relative error of the two different methods was less than 10%. When the structural measurement information was complete (all measurable), the error of ASO in identifying n9 was 7.52% (maximum error). The identification results of other parameters were less than 5%. The error of RREASO in identifying n9 was 5.13% (maximum error), and the other parameter identification results were also less than 5%. When the structural measurement information was incomplete (partially measurable), the maximum error of RREASO identification was 5.26%, and the error of all other parameters was less than 5%. The maximum error of ASO identification was 9.87%, except for n5, n7, and A1 which were greater than 5%. The remaining errors were all less than 5%. When the response information was partially measurable, the maximum error for RREASO identification was 5.3%, while the error recognized by ASO was 9.9%. The results show that the recognition efficiency of RREASO algorithm is better than ASO algorithm in terms of known quality and 10% noise. This method also has good parameter recognition ability for structures with more degrees of freedom. This is because the RREASO algorithm retains the characteristics of few ASO algorithm parameters and simple algorithm implementation. However, in the atomic search path selection, the RREASO algorithm does not add any complex operators in the original ASO algorithm. Therefore, the structure parameter identification method based on RREASO has great development potential and application prospect. The identification convergence process based on ASO and RREASO algorithms under both fully measurable and partially measurable response information conditions is shown in Figure 4.

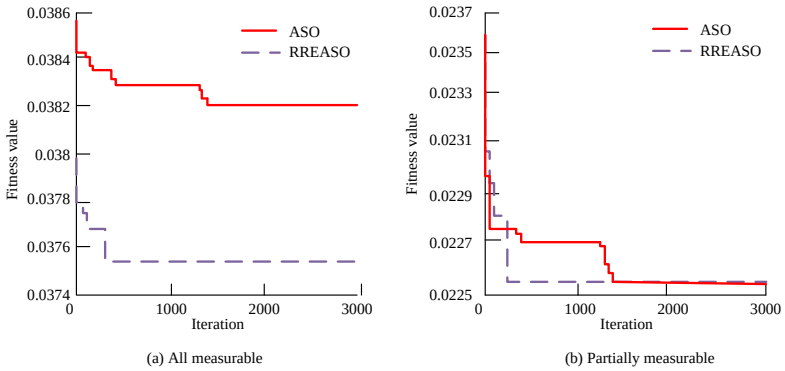

Figure 4: Identification convergence process of ASO and RREASO

From Figure 4, compared with the ASO, the RREASO had a faster recognition convergence speed, stronger ability to jump out of local optima, and global optimization ability. This advantage can save much computation time when dealing with higher dimensional problems. Therefore, the RREASO is more suitable for solving structural parameter identification problems with multiple degrees of freedom.

Secondly, to verify the effectiveness of combining substructure with RREASO in identifying large structural parameters with multiple degrees of freedom, numerical simulation experiments are conducted on parameter identification of a 25-story shear type structure. Assuming that the quality and damping of the simulation structure are known, the structure parameters to be identified are stiffness. Rayleigh damping matrix is used for damping. The system parameters of the simulation model are shown in Table 3.

Table 3: 25 layer shear structure system parameters

System parameter	Setting
Mass (kg)	1.20E+03
Stiffness (KN/m)	1.20E+06
First order damping ratio	5%
Second order damping ratio	5%
Structural response wave	EI Centro
Sampling interval	0.02s
Collect points	2688

When RREASO identifies each substructure, the termination condition is 500 iterations. When identifying the entire structure, the termination condition is 3000 iterations. The search space is 0.5-2 times the true value, and the number of atoms is set to 50. The identification error of the full structure and substructure is shown in Figure 5.

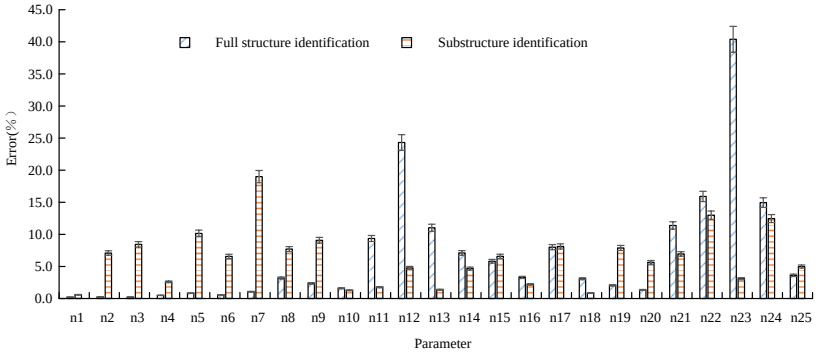

Figure 5: Identification error of full structure and substructure stiffness based on RREASO

From Figure 5, the maximum relative error for stiffness identification in the RREASO combined substructure identification method was 13%. Except for n5, n22, and n24, where the relative recognition error was greater than 10%, the relative recognition error of all other parameters was less than 10%. In the full structure parameter identification based on RREASO, the maximum relative error for stiffness identification was 43.1%, with relative errors greater than 10% for n12, n13, n21, n22, n23, and n24. The average error was 8.4% for all parameter identification. Compared with the full structure parameter identification method based on RREASO, the structural parameter identification results using RREASO combined with substructure identification method are better.

3.2 Application of structural parameter identification based on RREASO

To further verify the RREASO in identifying real structural parameters, the study applies the RREASO algorithm to the system parameter identification of a five-story metal frame structure vibration model. Two types of copper columns are selected for the experiment. The copper columns are connected to the aluminum alloy floor slab through L-shaped connectors and bolts to form a frame. The metal plate at the bottom of the frame is fixed on the vibration table, with a frame height of 30cm and a total height of 150cm. Each floor of the framework is connected by four copper columns to two aluminum

alloy floor slabs, forming a five-story framework. Five out of six acceleration sensors are arranged in the sensor support of each layer, and the other is arranged in the frame bottom plate to record the acceleration signal of the vibration table. The sensor support is fixed to the floor slab by bolts. The relevant parameters of the framework structure are displayed in Table 4.

Table 4: Relevant parameters of the five-story metal frame structure

Copper pillar type	Size(hxbxI)	Inter-layer theoretical stiffness(N/m)	Inter-layer mass	
A type of column	0.003mx0.030m×0.24m	47240	1-4 layers	7.2523 kg
Class II column	0.003mx0.014m×0.24m	22044	5 layer	6.5421 kg
			Young's modulus of copper(N/m²)	1.0×10l

The excitation equipment used in the study is a single degree of freedom electric servo vibration reduction platform. A sine sweep signal with a frequency ranging from 1Hz to 15Hz is used as the input signal. Its scanning rate is 0.5 octaves per minute (OCT/min). The accelerometer fixed at the bottom plate of the frame records the input signal. A part of the excitation signal is shown in Figure 6. The acquisition instrument is Donghua DH8303 dynamic signal acquisition instrument. The sampling frequency for acceleration time history is 200Hz.

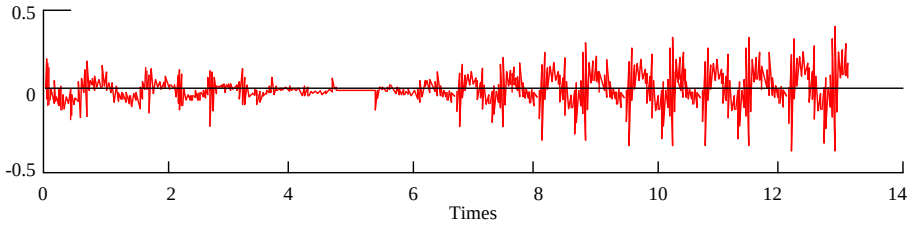

Figure 6: Time history curve of structural excitation acceleration

A total of six structural conditions are built to verify the recognition effect of the RREASO, as displayed in Table 5. The structural excitation remains consistent under each working condition.

Table 5: Testing conditions for frame structures

Working condition	Working conditions	Theoretical stiffness reduction
1	The copper columns used in the framework are all Class I columns	0
2	Replace the first layer of 4 columns with Class II columns	First layer reduction of 53.34%
3	Replace the 2nd floor of 4 copper columns with Class II columns	Second layer reduction of 53.34%
4	Replace the 3rd floor of 4 columns with Class II column	Third layer reduction of 53.34%
5	Replace the 4th floor of 4 columns with Class II columns	Fourth layer reduction of 53.34%
6	Replace the 5th floor of 4 columns with Class II columns	Fifth layer reduction of 53.34%

In Table 5, condition 1 shows that all copper columns used in the structure are Class I columns, and the structural state is non-destructive. In working condition 2, Class II columns are used to replace the four coppers columns on the first floor. In working condition 3, Class II columns are used to replace the four copper columns

on the second floor. In working condition 4, Class II columns are used to replace the four copper columns on the third layer. In working condition 5, Class II columns are used to replace the four copper columns on the fourth layer. In working condition 6, Class II columns are used to replace the four copper columns on the fifth floor. Based on the acceleration signals measured in the experiment, ASO and RREASO algorithms are used to identify the inter story stiffness of the frame structure. The identification results are shown in Figure 7.

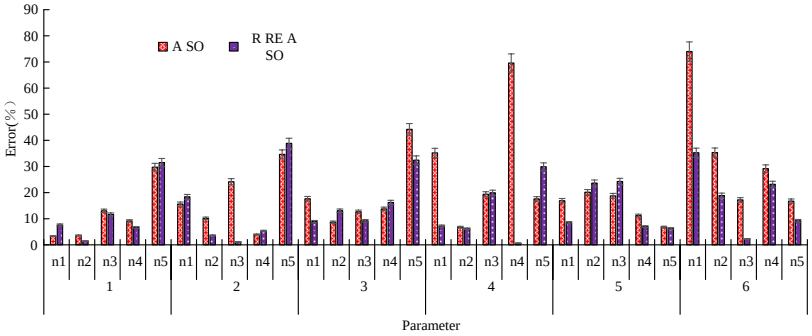

Figure 7: Real structure identification results under different working conditions

In Figure 7, the search space of both algorithms is 0.5-2.0 times the theoretical value of inter layer stiffness. The iterations are 1000. From Figure 7, in operating condition 1, the relative errors of using RREASO to identify n1, n2, and n4 were less than 10%, while the relative errors of identifying n3 and n5 were 11.6% and 31.9%, respectively. The ASO algorithm and RREASO recognition results were not significantly different. In working condition 2, the error in identifying n2, n3, and n4 using RREASO was less than 10%, while the error in identifying n3 using ASO was 24.2%. In working condition 3, the error of the RREASO recognition result for n1 was less than 10%. The ASO recognition result for n1 was 17.6%, which was 8.9% higher than the RREASO method. The recognition results of the ASO method for n2-n5 were not significantly different from those of the RREASO method. In working condition 4, the error of RREASO identification for n1, n2, and n4 was less than 10%, and the error of n3 identification result was less than 20%. The ASO recognition error for n4 was 69.6%, which deviated significantly from the theoretical value. In working condition 5, the recognition errors of RREASO for n1 and n4 were both less than 10%, while the ASO for n1 and n4 were 16.9% and 11.2%, respectively. In working condition 6, the RREASO identification errors for n1, n2, n3, and n5 were 35.3%, 18.9%, 2.3%, and 9.3%, respectively. The ASO for n1, n2, n3, and n5 were 74.0%, 35.3%, 17.2%, and 16.7%, respectively, and the recognition effect was lower than RREASO.

To verify the RREASO in identifying real structural damage, the stiffness reduction results identified by RREASO in condition 1 are used as the reference state. It is compared with the other five conditions. The stiffness reduction results identified by ASO and RREASO under various operating conditions are shown in Figure 8.

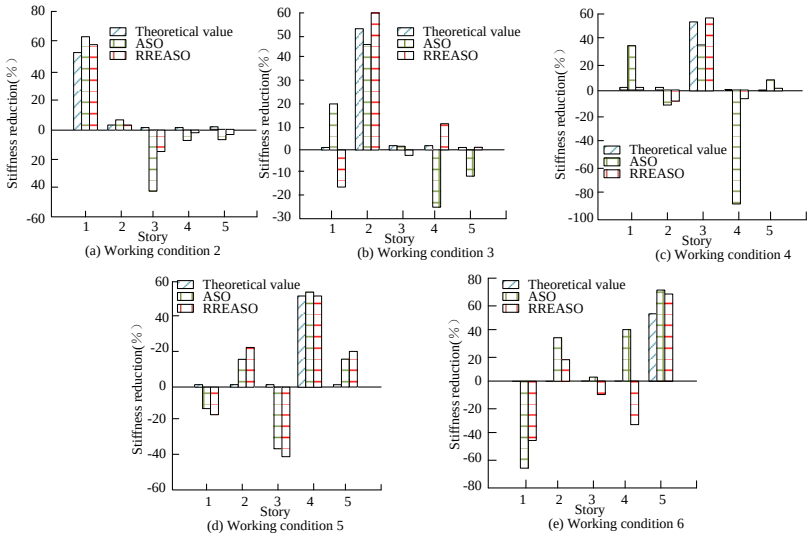

Figure 8: Identification results of stiffness reduction under various working conditions

From Figure 8 (a), in working condition 2, the theoretical stiffness reduction of the first layer was 53.3%. The stiffness reduction of the first and second layers identified by RREASO was 58.7% and 2.2%, respectively. The identification error was less than 10%, which was better than the ASO. The identification results of the third, fourth, and fifth layers showed a negative reduction in stiffness. It indicated no reduction in stiffness. From Figure 8 (b), in working condition 3, the theoretical stiffness of the second layer was reduced by 53.3%, the RREASO identification stiffness was reduced by 58.9%, and its identification relative error was about 10%, while the ASO identification stiffness was reduced by 47.4%. From Figure 8 (c), in working condition 4, the theoretical stiffness of the third layer was reduced by 53.3%, and the RREASO identification stiffness was reduced by 57.7%, with a relative identification error of only 8.2%. The relative recognition error of the other layers was less than 8%. The stiffness reduction of the third layer identified by ASO was 35.90%. From Figure 8 (d), in working condition 5, the theoretical stiffness of the fourth layer was reduced to 53.3%. RREASO reduced the recognition stiffness to 54.4%, while ASO reduced the recognition stiffness to 53.5%. The recognition results of the two algorithms are not significantly different. From Figure 8 (e), in working condition 6, the theoretical stiffness of the fifth layer was reduced to 53.3%. The RREASO reduced the recognition stiffness to 67.8%, while ASO reduced the recognition stiffness to 70.1%. The results of both methods in identifying the stiffness reduction of each layer are not very good, but RREASO has better recognition performance than ASO.

To further verify the effectiveness of the proposed method, the monitoring data from Bridge A is adopted. After 19 years of operation, the damage has accumulated, including concrete cracking, steel corrosion, pier damage, etc. The first maintenance and reinforcement project was carried out from July 2006 to February 2007. Specific reinforcement measures include replacement and reinforcement of closed sections, full bridge cable replacement, and bridge deck renovation, etc. The second repair was conducted form December 2008 to May 2009. Before the second maintenance, the structural health monitoring system with 15 acceleration sensors as the main component was designed for the bridge, so as to timely detect the structural damage leading to major disasters of the bridge, and improve the safety and reliability of the bridge. The structural dynamic response system in the structural health monitoring system fully recorded the vibration data of bridge A from the health state to the damage state (January 2008 to July 2008).

When evaluating the RREASO prediction performance, only 300 continuous data are intercepted. Among these 300 data samples, the first 200 data samples are used as the training set for predicting the next data point (201 data point) (which is also known as one-step prediction). The second data to 201 data are used as the training set for predicting the next data point (202 data point), and so on. The one-step prediction is repeated 100 times. The prediction results of environmental vibration data in the damage state are shown in Figure 9.

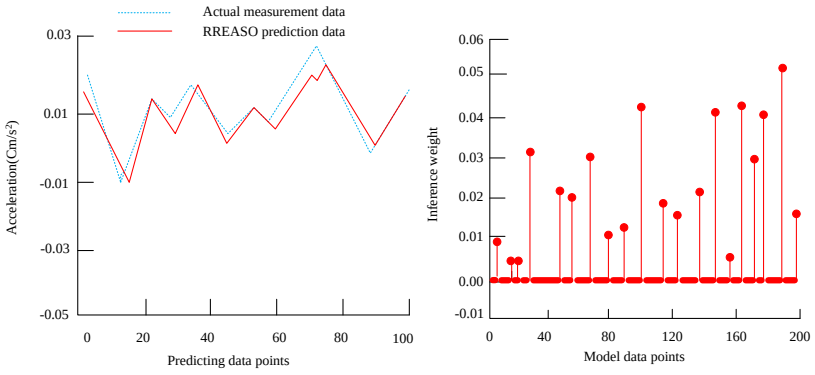

Figure 9: Prediction results of environmental vibration data in the damaged condition

In Figure 9, the vibration data in the damaged condition is from acceleration sensor # 1 during 01:00-02:00 on July 31,2008. Figure 9 (a) shows the prediction results of the RREASO algorithm on the environmental vibration data in the damaged state. The RMSE of SBL was 0.0116. From Figure 9 (b), most of the inferred weights were zero, and the number of non w (i. e. w in equation 2) was only 44. The results show that the prediction results are more consistent with the measured data, and the research algorithm is feasible.

4 Discussion

The numerical simulation results showed that when all the response information was measurable, the maximum relative error of ASO and RREASO was 7.5% and 5.1%, while the recognition result of other parameters was also less than 5%. When the response information was measurable, the maximum error of RREASO and ASO

was 5.3% and 9.9% respectively. The results show that the maximum identification error and mean error of RREASO are smaller than the ASO identification results, whether the test information is complete or not. The result is in line with the results of Han et al. [15] in the parameter identification study for the speed regulation system of pumped storage units. The ASO is influenced by the complex scene structure when improving the global search power of the initial population, leading to increased identification error. Compared with the ASO method, the parameter identification results based on the RREASO method were better, and the performance of the RREASO algorithm was somewhat improved. This is because the RREASO algorithm retains a small number of ASO algorithm parameters and simple algorithm implementation characteristics. In the atom search path selection, the RREASO algorithm does not add any complex operators to the original ASO algorithm, which can identify more complex building structures. In the identification method using RREASO binding substructures, the maximum relative error of stiffness identification was 13%, and less than 10% except for n5, n22, and n24. In the RREASO-based full structure parameter identification, the maximum relative error of stiffness identification was 43.1%, with n12, n13, n21, n22, n23, and n24 all greater than 10%. The results show that when identifying the low-level structure parameters, the whole structure parameters based on RREASO is more effective. The stiffness of the upper part of the structure becomes worse. When using the RREASO-based substructure identification method, the identification results of each substructure are roughly the same and the recognition effect is good. This result is consistent with the multi-objective binary results based on ASO algorithm proposed by Asna et al. [16] for the planning of fast charging stations for electric vehicles. In general, compared with the RREASO-based full structure parameter identification method, the structural parameter identification results using RREASO combined with substructure identification method are better, because the convergence speed of the algorithm is improved when the method is used for the construction parameter identification target.

5 Conclusion

With the development of large-scale, complex and intelligent infrastructure facilities, the civil engineering structure damage is becoming increasingly prominent. Accordingly, starting from the idea of increasing the randomization features of the algorithm and maintaining population diversity, this paper combined substructure techniques to introduce roulette wheel selection strategy, random walk, and elite selection strategy into the ASO algorithm, and improved the ASO algorithm. The numerical simulation experimental results showed that the parameter identification results of RREASO algorithm were less than 5%, which was better than ASO algorithm. It indicated that the global search ability of the improved algorithm and the identification accuracy were improved. The improved algorithm was applied to the structural parameter identification of the five-layer metal frame structure model. The experimental results showed that the identification error of RREASO algorithm was less than 10%, the identification stiffness was reduced to 58.85%, and the relative error was about 10%, which was better than ASO algorithm. The improved algorithm was effective and feasible for the identification of building structure damage. First of all, the improved ASO algorithm has been improved compared with the original ASO algorithm. The identification accuracy of the algorithm is higher than other methods. However, in terms of computational efficiency, it still needs to be improved compared with other methods. In addition, the ASO algorithm can be applied to finite element model correction in structural dynamics in the future. Finally, the proposed method is only well verified in numerical simulation and small-scale shear frame test model parameters identification. In the future, attempts can be made to identify more complex structural model parameters, and even actual engineering structural parameters can be identified.

Data availability statement

All data generated or analyzed during this study are included in this article.

Disclosure statement

There’s no conflict of interest in this research.

Reference

[1] K. Yang, Y. Ding, and H. Jiang, “Deep learning-based bridge damage identification approach inspired by internal force redistribution effects,” Structural Health Monitoring, vol. 23, no. 2, pp. 714-732, 2024. https://doi.org/10.1177/14759217231176050

[2] A. Bilotta, A. Morassi, and E. Turco, “Damage identification for steel-concrete composite beams through convolutional neural networks,” Journal of Vibration and Control, vol. 30, no. 3-4, pp. 876-889, 2024. https://doi.org/10.1177/10775463231152926

[3] A. Sivasuriyan, D. S. Vijayan, and W. Górski, “Practical implementation of structural health monitoring in multi-story buildings,” Buildings, vol. 11, no. 6, pp. 263-2680, 2021. https://doi.org/10.3390/buildings11060263

[4] H. M. Dinh, T. Nagayama, and Y. Fujino, “Structural parameter identification by use of additional known masses and its experimental application,” Structural Control and Health Monitoring, vol. 19, no. 3, pp. 436-450, 2022. https://doi.org/10.1002/stc.444

[5] E. García-Macías, I. A. Hernández-González, and E. Puertas, “Meta-model assisted continuous vibration-based damage identification of a historical

rammed earth tower in the Alhambra complex," International Journal of Architectural Heritage, vol. 18, no. 3, pp. 427-453, 2024. https://doi.org/10.1080/15583058.2022.2155883

[6] G. Bandewad, K. P. Datta, B. W. Gawali, and S. N. Pawar, "Review on discrimination of hazardous gases by smart sensing technology," Artificial Intelligence and Applications, vol. 1, no. 2, pp. 86-97, 2023. https://doi.org/10.47852/bonviewAIA3202434

[7] Z. Zhang, and C. Sun, "Structural damage identification via physics-guided machine learning: a methodology integrating pattern recognition with finite element model updating," Structural Health Monitoring, vol. 20, no. 4, pp. 1675-1688, 2021. https://doi.org/10.1177/1475921720927488

[8] Y. Lu, C. Z. Zhao, and J. Q. Huang, "The timescale identification decoupling complicated kinetic processes in lithium batteries," Joule, vol. 6, no. 6, pp. 1172-1198, 2022. https://doi.org/10.1016/j.joule.2022.05.005

[9] A. M. Fallah, E. Ghafourian, and L. Shahzamani Sichani, "Novel neural network optimized by electrostatic discharge algorithm for modification of buildings energy performance," Sustainability, vol. 15, no. 4, pp. 2884-2901, 2023. https://doi.org/10.3390/su15042884

[10] F. Elghaish, S. Talebi, and E. Abdellatef, "Developing a new deep learning CNN model to detect and classify highway cracks," Journal of Engineering, Design and Technology, vol. 20, no. 4, pp. 993-1014, 2022. https://doi.org/10.1108/JEDT-04-2021-0192

[11] N. Bao, T. Zhang, R. Huang, S. Biswal, J. Su, and Y. Wang, "A deep transfer learning network for structural condition identification with limited real-world training data," Structural Control and Health Monitoring, vol. 2023, pp. 1-18, 2023. https://doi.org/10.1155/2023/8899806

[12] N. Malekghaini, F. Ghahari, and H. Ebrahimian, "A two-step FE model updating approach for system and damage identification of prestressed bridge girders," Buildings, vol. 13, no. 2, pp. 420-438, 2023. https://doi.org/10.3390/buildings13020420

[13] M. F. Funari, A. E. Hajjat, M. G. Masciotta, D. V. Oliveira, and P. B. Lourenço, "A parametric scan-to-FEM framework for the digital twin generation of historic masonry structures," Sustainability, vol. 13, no. 19, pp. 11088-11105, 2021. https://doi.org/10.3390/su131911088

[14] X. Han, Y. Wu, Y. Wang, S. Liu, and C. Liu, "Application of ASO algorithm in parameter identification of photovoltaic cells," 2022 IEEE International Conference on Mechatronics and Automation (ICMA), vol. 5, no. 6, pp. 1866-1870, 2022. https://doi.org/10.1109/ICMA54519.2022.9856201

[15] L. Wang, L. Zhang, W. Zhao, and X. Liu, "Parameter identification of a governing system in a pumped storage unit based on an improved artificial hummingbird algorithm," Energies, vol. 15, no. 19, pp. 69666970, 2022. https://doi.org/10.3390/en15196966

[16] M. Asna, H. Shareef, M. A. Muhammad, L. Ismail, and A. Prasanthi, "Multi-objective quantum atom search optimization algorithm for electric vehicle charging station planning," International Journal of Energy Research, vol. 46, no. 12, pp. 17308-17331. https://doi.org/10.1002/er.8399

[17] E. Eker, M. Kayri, S. Ekinci, and D. Izci, "A new fusion of ASO with SA algorithm and its applications to MLP training and DC motor speed control," Arabian Journal for Science and Engineering, vol. 21, no. 46, pp. 3889-3911, 2021. https://doi.org/10.1007/s13369-020-05228-5

[18] C. Bi, Q. Tian, H. Chen, X. Meng, H. Wang, W. Liu, and J. Jiang, "Optimizing a multi-layer perceptron based on an improved gray wolf algorithm to identify plant diseases," Mathematics, vol. 11, no. 15, pp. 3312-3327, 2023. https://doi.org/10.3390/math11153312

[19] E. F. Tsani, and D. Suhartono, "Personality identification from social media using ensemble BERT and RoBERTa," Informatica, vol. 47, no. 4, pp. 1-8, 2023. https://doi.org/10.31449/inf.v47i4.4771